PREDICTED INFECTION RISK FOR AEROSOL TRANSMISSION OF SARS-COV-2

Martin Kriegel[1], Udo Buchholz[2], Petra Gastmeier[3], Peter Bischoff[3], Inas Abdelgawad[4], Anne Hartmann[1]

[1] Technical University of Berlin, Hermann-Rietschel-Institut

[2] Robert-Koch-Institute, Department for Infectious Disease Epidemiology

[3] Charité-University Medicine Berlin, Institute for Hygiene and Environmental Medicine

[4] Public Health Department Berlin Spandau

Address for correspondence:

Prof. Dr.-Ing. Martin Kriegel

Hermann-Rietschel-Institut

TU Berlin

m.kriegel@tu-berlin.de

Author contributions:

MK extended the existing models and performed the calculation. UB and IA supplied the data for retrospective analysis to validate the model. PG, PB, UB and IA evaluated the results from a medical point of view. AH performed the literature research and the review of the models and calculations. MK and AH drafted the manuscript. All authors contributed to the interpretation of the results, critically revised the paper and agreed on the final version for submission.

NOTE: This preprint reports new research that has not been certified by peer review and should not be used to guide clinical practice.

1   **Abstract**

2   Currently, airborne transmission is seen as the most important transmission path for SARS-

3   CoV-2. In this investigation, a models of other researchers with the aim to predict an infection

4   risk for exposed persons in a room through aerosols emitted by an infectious case-patient

5   were extended. As a novelty – usually neglected – parameters or boundary conditions, namely

6   the non-stationarity of aerosol and the half life of aerosolized virus, were included and a new

7   method for determining the quanta emission rate based on measurements of the particle

8   emission rate and respiratory rate at different types of activities was implemented.

9   As a second step, the model was applied to twelve outbreaks to compare the predicted

10   infection risk with the observed attack rate. To estimate a "credible interval" of the predicted

11   infection risk the quanta emission rate, the respiratory rate as well as the air volume flow were

12   varied.

13   In nine out of twelve outbreaks, the calculated predicted infection risk via aerosols was found

14   to be in the range the attack rate (with the variation of the boundary conditions) and reasons

15   for the observed larger divergence were discussed.

16   The validation was considered successful and therefore, the use of the model could be

17   recommended to predict the risk of an infection via aerosols in given situations. Furthermore,

18   appropriate preventive measures can be designed.

19

20   **Introduction**

21   The respiratory route is the main mode of transmission for the virus causing COVID-19

22   (SARS-CoV-2) [1, 2, 3]. The virus is transported on particles that can enter the respiratory

23   tract. Whereas larger particles (droplets) are only able to stay in the air for a short time and

24   just in the near field (approx. 1.5 m), because they settle down quickly, smaller particles

25   (called aerosols) are also concentrated in the near field and in addition can follow the air flow

26   and cause infections in the far field. Epidemiologically, short-range transmission (through

27   aerosols or droplets) is distinguished from long-range transmission (aerosol).

28   In order to perform an infection risk assessment for the airborne transmission in the far field

29   and to introduce appropriate preventive measures, it would be necessary to know the amount

30   of aerosols produced by an infected person during various activities, how many viruses stick

31   to the aerosols and how many viruses are necessary to cause an infection. However, this

32   information is usually available very late during the course of a pandemic, if it can be

33   determined at all. Another well-known approach is to use retrospective analysis of infection

34   outbreaks that are very probably due to far field transmission to determine a virus-laden

35   aerosol concentration. Exposed people have inhaled the virus-laden aerosols according to

36   their respiratory volume flow. The approach presented here corresponds to a combination of

37   known measured source rates of respiratory aerosols at different activities and the

38   retrospective analysis of previous infection incidents with the aim to calculate a predicted

39   infection risk via aerosols and to calculate the necessary air volume flow to reduce the risk of

40   COVID-19 infections.

41

42   **State of the Art**

43   The so-called aerosols (liquid or solid particles in a dispersed phase with a fluid) as well as

44   droplets differ by size. The particles, which are transported in a fluid over a longer distance,

45   are called aerosols. Droplets are stronger influenced by gravitation and are depositing more

46   rapidly. Depending on the fluid velocity the size of particles, which can be transported in air

47   for a longer distance, is different. In internal spaces with typical air velocities of up to 0.2 m/s

48   particles smaller than 10 μm will be distributed by air very well, with a higher air velocity

49   larger particles may be transported in air as well.

50 SARS-CoV-2 was found to be transmitted via close contact as well as over distance in

51 internal spaces, whereby in distant transmission so-called super-spreading events are more

52 probable [1, 2, 4].

53 In 1978, Riley et al. [5] evaluated a measles outbreak in a suburban elementary school. Based

54 on the number of susceptible persons (S), which have been infected (D) during each stage of

55 infection, the risk (P) for an infection in this stage has been calculated regarding equation (1).

56 Therefore, the risk for an infection has been defined as the percentage of infected persons

57 from the number of pupils not already infected or vaccinated.

$$P = \frac{D}{S} \tag{1}$$

58 A Poisson-distribution of the risk of infection has been assumed as well as a stationary and

59 evenly distributed concentration of the pathogens in the room air. Equation (2) shows the

60 Poisson-distribution.

$$P = 1 - e^{-\lambda} \tag{2}$$

61 Therefore, Wells defined in 1955 [6] a size called quantum as the number of emitted

62 infectious units, where the probability to get infected is $1 - e^{-1} = 63.2\%$. Hence, a quantum

63 can be seen as a combination of the amount of emitted aerosols with the virus transported on

64 them and a critical dose, which may result in an infection in 63.2 % of the exposed persons.

65 Using the quantum concept as well as equation (2) has been combined by Riley [5] to

66 equation (3).

$$P = 1 - e^{-I \cdot q \cdot Q_b \cdot t / Q} \tag{3}$$

67 In equation (3), the number of infectious persons (I), the quanta emission rate depending on

68 the activity (q), the pulmonary ventilation rate of exposed susceptible persons (Q_b), the

69 duration of stay (t) and the volume flow of pathogen free air (Q) was used. The quotient q/Q

70 represents the quanta concentration.

71   In poorly ventilated rooms, the assumption of a stationary concentration of quanta is not

72   justified, because of the long time, which is necessary until the stationary concentration is

73   reached. The normalized time-dependent concentration process can be calculated according to

74   equation (4) and is shown in Figure 1. How rapidly the concentration of a human emitted

75   contamination in a room raises depends on the air exchange rate (ACH) and the time (t). This

76   relative concentration (c_{rel}) can be seen as an increase in the concentration compared to the

77   volume flow.

$$c_{rel} = 1 - e^{-ACH \cdot t} \tag{4}$$
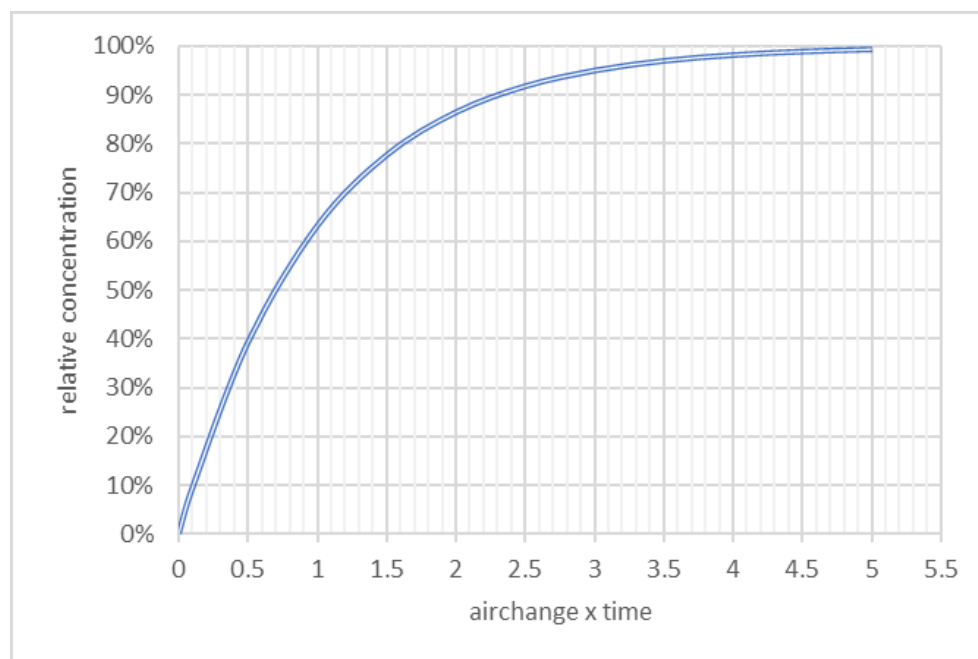
78

79

80   *Figure 1: Relative concentration curve as a function of air exchange rate and time.*

81

82   In all published studies identified ideal mixing ventilation was assumed, which means that

83   aerosols are evenly distributed in the room air. To avoid this assumption Noakes and Sleigh

84   [7] divided the room air into different zones, which are themselves considered to be well

85   mixed and have a uniform concentration. This should make it possible to calculate local

86   differences in concentration and thus locally differing infection risks. Furthermore, other

87 studies, which focus on the unsteady conditions mostly use the boundary condition of a

88 starting concentration of $c(t = 0) = 0 \frac{quanta}{m^3}$. Gammaitoni and Nucci [8] implemented the

89 starting condition of $c(t = 0) = c_0$ as well as the number of exposed susceptible people,

90 which may also change over time depending on their immune status.

91

92 To estimate the risk of infection in a given setting by a given infectious person with the

93 Wells-Riley-equation either the quanta emission rate or the P have to be known. In the

94 beginning of an epidemic, both values are unknown. Dai and Zhao [9] correlated and

95 calculated q for SARS-CoV-2 based on the basic reproduction number (R_0) known from

96 former outbreaks of MERS, tuberculosis, Influenza as well as SARS-CoV-1 and published

97 the equation (5). If R_0 is known, q can be estimated as proposed by Dai and Zhao [9]. For

98 SARS-CoV-2 the average basic reproduction number has been estimated to be 3.28 [10], 3.32

99 [11] and 3.77 [12].

$$q = -30.27958 - 44.81536 \cdot R_0 + 19.67934 \cdot R_0^2 \qquad (5)$$

100

101 In various studies of infection occurrences associated with SARS-CoV-2, q was determined

102 using the Wells-Riley equation. Different authors [9, 13] found a range of 22 to 61 quanta/h

103 with an assumed low activity (breathing, speaking) and values of 341 to 1190 quanta/h when

104 singing.

105

106 The virus can be transported on particles in air and the emission of aerosols can be used as an

107 indicator for the emission of virus, but a correlation between q and the aerosol emission rate

108 (E) has not been investigated so far. In measurements at the Hermann-Rietschel-Institute

109 (HRI) of Technical University of Berlin [14, 15] the particle emission rates during breathing,

110 speaking, coughing as well as singing was measured. During breathing through the nose about

111 25 particles/s was emitted and during coughing about 13,700 particles/cough, whereas it can

112 be seen that depending on the activity a wide range of particle emission rates can be found.

113 The transmission of a pathogen via aerosols is also influenced by the stability of the virus in

114 the environment. In an experimental study van Doremalen et al [16] measured the decrease of

115 infectious virus in air and on different surfaces and compared SARS-CoV-1 and SARS-CoV-

116 2. Under the given conditions, the half-life of SARS-CoV-2 as well as SARS-CoV-1 was

117 about 1.1 h.

118 The longer aerosols stay in the room air the proportion of inactivated virus is increasing. The

119 age of air is depending on the airflow as well as the position of the source of pollutants. At

120 each point in the room, a local age of air can be calculated. The age of air (τ_n) can be used as a

121 measure to evaluate the air quality. For an ideal mixing ventilation, the mean age of air is

122 equal to the nominal time constant, which can be calculated using equation (6) as the quotient

123 of the room volume (V) and the air volume flow (Q).

$$\tau_n = \frac{V}{Q} \tag{6}$$

124 Besides the number of emitted pathogen-laden aerosols, the number of inhaled pathogens is

125 playing an important role as well with regard to the assessment of the risk of infection. The

126 pulmonary ventilation rate may differ with different activities. Gupta et al. [17] performed a

127 study with 25 healthy adults and found a sine wave for mere breathing, but a more constant

128 volume flow during talking.

129 In measurements with athletes as well as sedentary persons a maximum volume flow for the

130 athletes of 200 l/min (12 m³/h) was found by Córdova and Latasa [18].

131 To measure the airflow without movement restrictions, a helmet was used by Jiang et al. [19]

132 in 32 subjects (16 males, 16 females) during speaking with different volumes as well as

133 during singing.

134   A comparison between a machine-learning based model and measurements of respiratory rate

135   was performed by Dumond et al. [20].

136   As a conclusion, the following average values can be used for adults:

137   - low activity (breathing while lying): 0.45 m^3/h [19]

138   - low activity (breathing while sitting, standing or talking): 0.54 m^3/h [19, 20]

139   - singing: 0.65 m^3/h [21]

140   - mid activity (physical work): 0.9 m^3/h [20]

141   - sports: 1.2 m^3/h [18, 20]

142   For children, the lung volume is smaller. Therefore, the respiratory rate for children aged 14

143   can be assumed to be 0.45 m^3/h for low activity (breathing while sitting, standing, talking)

144   [22].

145

146   **Methods**

147   **Extension of the Wells-Riley equation for calculating the Predicted Infection Risk via**

148   **Aerosols (PIRA)**

149   The Wells-Riley equation can be summarized as equation (7). To calculate the predicted

150   infection risk via aerosols (PIRA) in the far field of a room the concentration of quanta (c(t))

151   and the respiratory rate (Q_b) has to be known. The integration of c(t) can be understood as the

152   amount of particles inhaled per m^3/h. With Q_b the number of inhaled quanta can therefore be

153   calculated.

$$PIRA = 1 - e^{(-\int [c(t)]\cdot Q_b)} \tag{7}$$

154   Equation (5) can be used for the definition of the quantum emission. This leads to a quanta

155   emission rate of q = 40 1/h at an assumed mean R_0 = 3.35. The mathematical approximation

156   presented by Dai und Zhao [9] can be optimized by equation (8), see Figure 2. For Figure 2

157   the quanta emission rate has been correlated with R_0 of tuberculosis [23, 24], Influenza [23,

158   25], MERS [26, 27] and SARS-CoV [23, 28].

159   Equation (8) results in q = 139 1/h for an assumed mean R_0 = 3.35. Because of the high

160   variance of the q as well as R_0 given in the currently available literature the difference

161   between the q calculated regarding equation (5) and equation (8) seems reasonable.
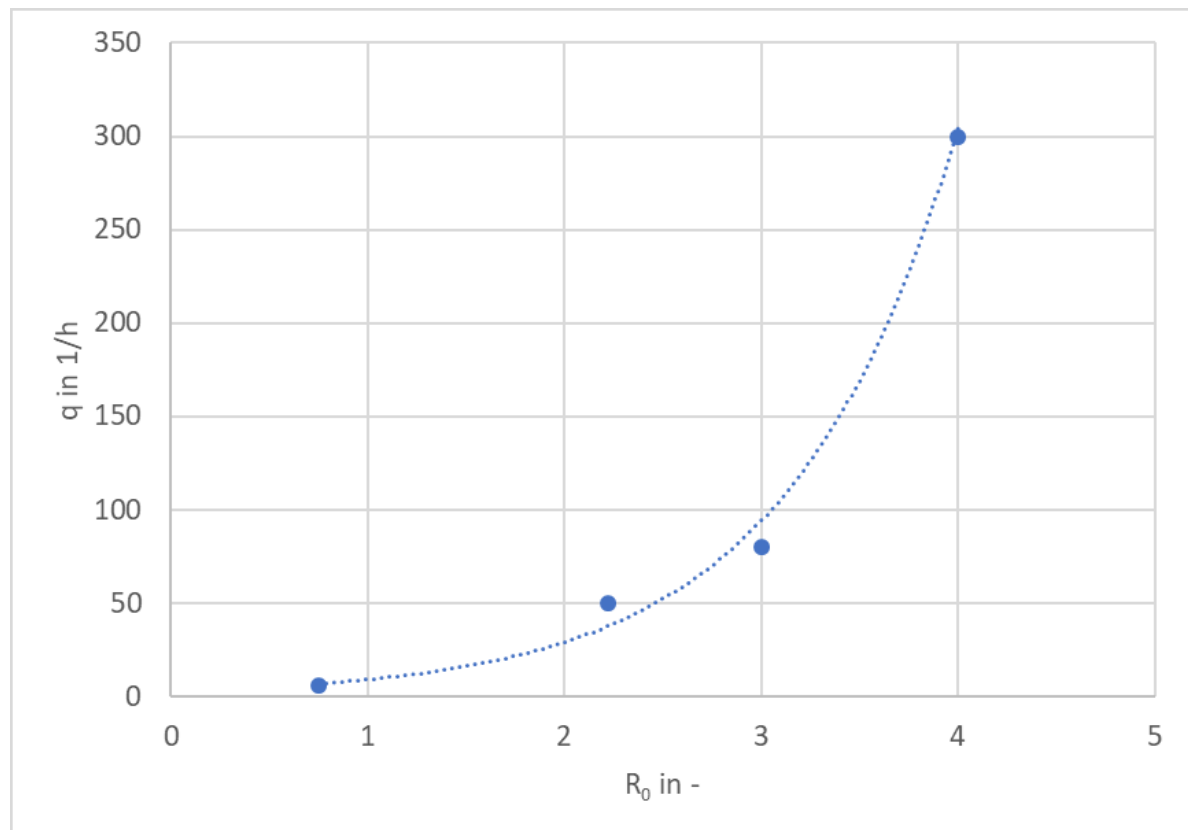

162   *Figure 2: Relationship between quanta emission rate and R_0 according Dai and Zhao [9]*

163

$$q_0 = 2.7618 \cdot (e^{1.1761 \cdot R_0} - 1) \qquad (8)$$

164

165   q is influenced by the activity of the person as was shown by Buonanno et al. [29]. Therefore,

166   the measured aerosol emission rates E [14, 15] were correlated with the calculated quanta

167   emission rates influenced by the activity q_a by equation (9). For low-activity (breathing,

168   talking, sitting, standing) a basic volume flow $Q_{b,o}$ and normal activity = low activity

169   (breathing, talking, sitting, standing) with a basic emission rate of E_0 was used. Furthermore,

170   the basic q (q_0) was calculated with usage of R_0 regarding equation (8). With these

171   specifications q_a can be calculated.

$$q_a = q_0 \cdot \frac{E}{E_0} \cdot \frac{Q_b}{Q_{b,0}} \tag{9}$$

$$Q_{b,0} = 0.54 \frac{m^3}{h}; \qquad E_0 = 100 \frac{P}{s} \, [15]$$

172

173   The effect of e.g. mouth-nose protection can be considered by using their filtration efficiency

174   (F_{MNS}) like in equation (10) which however will not be further considered in the following.

$$q_{a,MNS} = F_{MNS} \cdot q_a \tag{10}$$

175

176   It is known that the infectivity of an infected person depends on the disease progression over

177   time [30]. This is shown qualitatively in Figure 3. With a simplified mathematical approach,

178   this can be integrated into the quanta source rate. An equation could be implemented to take
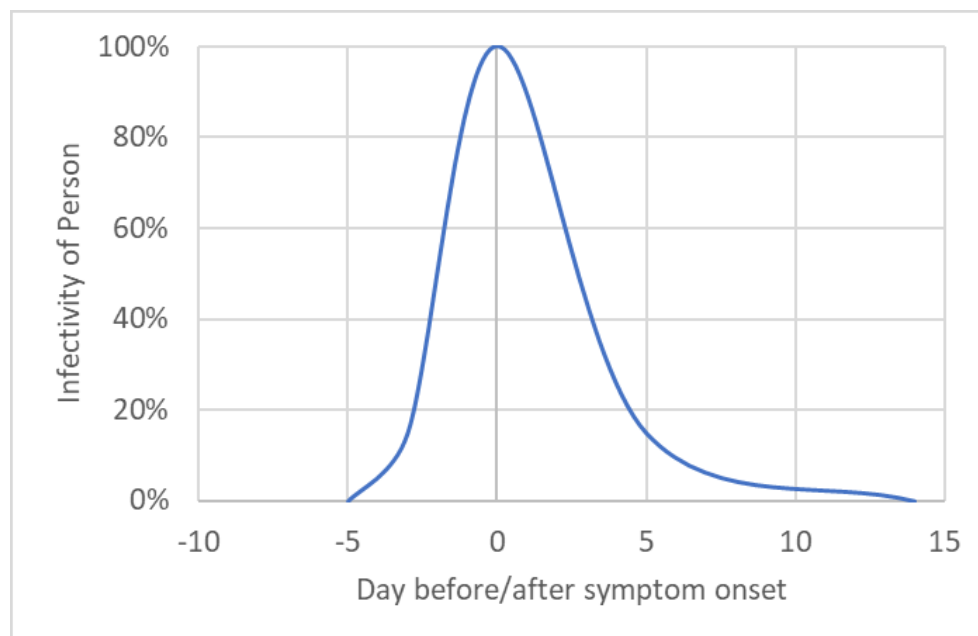
179   this into account.

180

181   *Figure 3: Infectivity depending on the disease progression*

182

183   Under experimental conditions, the half-life of virus was measured as 1.1 h [16]. Thus, the

184   number of emitted infectious quanta at time t ($q_a(t)$) is calculated according to equation (11).

$$q_a(t) = q_a \cdot e^{(-0.5776 \cdot t)} = q_a \cdot e^{\left(-\frac{361}{625} \cdot t\right)} \tag{11}$$

185   The concentration of quanta during the increase $c_I(t)$ can be calculated according to equation

186   (12) with the number of infectious persons (n).

$$c_I(t) = \frac{q_a(t)}{Q} \cdot n \cdot \left(1 - e^{(-ACH \cdot t)}\right) \tag{12}$$

187   An additional case is considered that if the time t is longer than the age of the air τ_n, most of

188   the virus-laden aerosols have left the room with the exhaust, before the inactivation can take

189   place. Therefore, this concentration during the steady state situation is called $c_\tau(t)$.

$$q_{a,\tau} = q_a \cdot e^{(-0.5776 \cdot \tau_n)} \tag{13}$$

$$c_\tau(t) = \frac{q_{a,\tau}}{Q} \cdot n \cdot \left(1 - e^{(-ACH \cdot t)}\right) \tag{14}$$

190   with τ_n regarding equation (6)

191

192   For calculating the risk of infection the unsteady concentrations c_I and c_τ has to be used, to

193   include the time-dependent increase in concentration and to include the time-dependent

194   viability of the virus, otherwise the result could be overestimated or underestimated.

195   For equation (7) the integration of $c_I(t)$ and $c_\tau(t)$ is necessary.

$$C_I = \int_0^t c_I(t)$$

$$= \frac{q_a \cdot \left(390625 \cdot ACH - \left((390625 \cdot ACH + 225625) \cdot e^{ACH \cdot t} - 225625\right) \cdot e^{-ACH \cdot t - \frac{361}{625} \cdot t}\right)}{Q \cdot (225625 \cdot ACH + 130321)} \tag{15}$$

$$C_\tau = \int_\tau^{t \geq \tau_n} c_\tau(t) = \frac{q_{a,\tau} \cdot e^{-ACH \cdot (t + \tau_n)} \cdot \left(ACH \cdot (t - \tau_n) \cdot e^{ACH \cdot (t + \tau_n)} - e^{ACH \cdot t} + e^{ACH \cdot \tau_n}\right)}{Q \cdot ACH} \tag{16}$$

196

197   The Predicted Infection Risk via Aerosols can be calculated by equation (17) and (18).

$$PIRA = 1 - e^{(-(C_I(t=\tau)+C_\tau)\cdot Q_b)} \qquad t > \tau_n \tag{17}$$

$$PIRA = 1 - e^{(-(C_I)\cdot Q_b)} \qquad t \leq \tau_n \tag{18}$$

198

199   For the calculation of PIRA the following assumptions must be considered:

200   • the aerosols are ideally mixed in the room

201   • the near field (up to approx. 1.5 m distance from the emitting person) can contain a

202   much higher virus-laden aerosol concentration

203   • the air, which is introduced into the room, is free of virus-laden aerosols (e.g. outside

204   air)

205   • no deposition of small particles is considered, because the settling time is longer than

206   the stability of the virus and the deposition rate would therefore be substantially

207   smaller than the inactivation

208   • the concentration of aerosols at the beginning is 0

209   **Results**

210   The PIRA calculation model was validated by using parameters of several known outbreaks

211   during the SARS-CoV-2 pandemic. Twelve different scenarios either scientifically published

212   or registered by the local health authorities were selected (A-L). The boundary conditions for

213   the calculations of these situations can be found in Table 1.

214 *Table 1: Boundary conditions of SARS-CoV-2 outbreaks for the retrospective calculation of PIRA*

	A	B	C	D	E	F	G	H	I	J	K	L
V in m³	3000	1200	60*	630	254	830	180	150	150	47	170	60***
n	1	1	1	1	1	1	1	1	1	1	1	1
q_a in 1/h	232	4213	139	139	139	4213	116	116	139	139	139	139
Q_b in m³/h	0.9	0.65	0.54	0.54	0.54	0.65	0.45	0.45	0.54	0.54	0.54	0,54
Q in m³/h	1600	200*	200*	4000**	50*	200*	1500*	1500*	400*	75	200*	1260***
exposure time t in h	8	2.5	1.66	8	1.5	2.5	4.5*****	1.5*****	4.5*****	1.2	2	11
Attack Rate**** in %	26%	91%	34%	5%	58%	87%	10%	6%	43%	45%	17%	63%

*due to partly missing information, assumptions were made, especially for window ventilation. The assumptions are based on information from the persons involved on how the windows were opened and closed in combination with weather data at the time.

** It was assumed that the local regulations for fresh air supply were fulfilled.

***Geometry and Ventilation Rate due to [31]

****Attack Rate was simplified as percentage of persons infected. No separation regarding infection attack rate (measured serologically) and illness attack rate (persons with symptoms or laboratory-confirmed) was performed.

***** It was assumed that a school lesson lasts 45 minutes.

	Setting	Country	Remarks
A	Slaughterhouse [32]	Germany	
B	Choir rehearsal Berlin	Germany	not yet scientifically published, investigated by Robert-Koch-Institute
C	Bus Tour [33]	China	
D	Call Center [34]	Korea	The attack rate is mentioned as 43 % in the publication. However, the infection occurred almost exclusively on one half of the 11th floor. The local attack rate is therefore actually significantly higher. In Table 1 an attack rate of 5% was given, because only persons who had shown symptoms were quarantined. If one includes the persons who showed symptoms up to and including 04.02., the attack rate is 5 %.
E	Club Meeting	Germany	not yet scientifically published, investigated by Robert-Koch-Institute
F	Choir rehearsal Skagiq [13]	USA	
G	School Berlin 1	Germany	not yet scientifically published, investigated by Public Health Department Berlin Spandau
H	School Berlin 2	Germany	not yet scientifically published, investigated by Public Health Department Berlin Spandau
I	School Israel [35]	Israel	
J	Restaurant [1, 36]	China	
K	Meeting	Germany	not yet scientifically published, investigated by Robert-Koch-Institute
L	Aircraft [37]	-	

215

216   The infection events used for the validation of the model are shown in Table 1 with the

217   necessary parameters for the calculation. In the following, the comparison between the

218   documented Attack Rate (AR) and the PIRA is drawn.

219   The q used here was calculated according to equation (9) with the assumption that the cases

220   emitted particles as measured in [14, 15]. Due to the high spread of the particle emission E

221   and the unknown proportions of breathing, speaking, singing and shouting as well as the

222   respiratory volume flows, simplified a-priori assumptions were made. To take into account

223   the effects of the uncertainties regarding q, Q_b and especially with window ventilation on Q,

224   these values were further varied - q by +/- 20%, Q_b by +/- 20% and Q by +/- 50%,

225   individually and in combination, which then lead to a minimum PIRA and maximum PIRA.

226   Figure 4 presents PIRA and the minima and maxima calculated with the different variants.
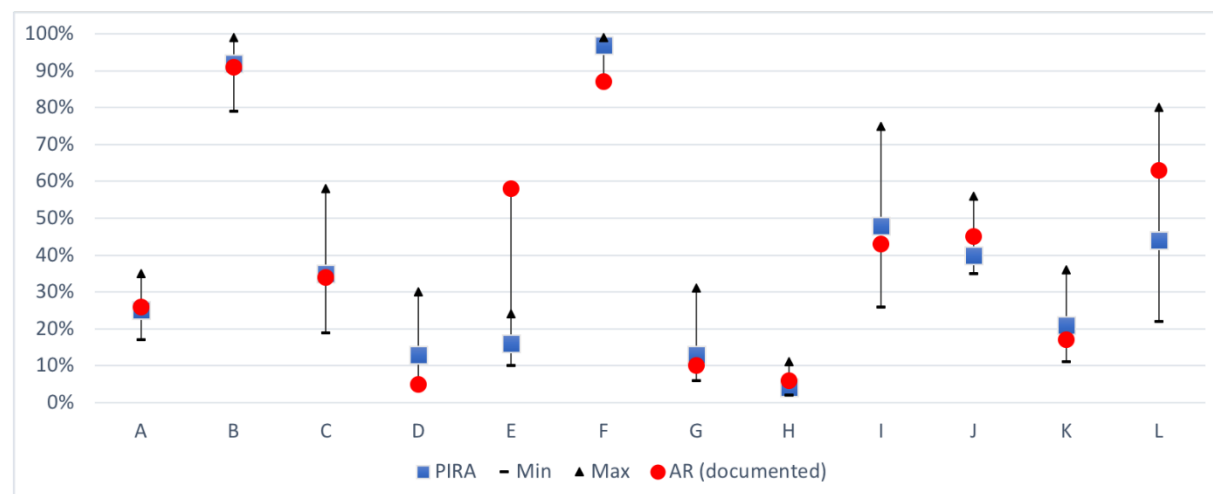
227   The red dots show the documented AR.

Figure 4: Comparison between PIRA with the variants Min and Max to the documented AR

assuming that all cases were caused by long-range transmission

232   In nine out of twelve outbreaks, the attack rate lies in the Min Max values of the calculated

233   PIRA (see Table 2).

234 *Table 2: Results of the Calculation of PIRA and comparsion with the documented AR*

	A	B	C	D	E	F	G	H	I	J	K	L
PIRA	25%	92%	35%	13%	16%	97%	13%	4%	48%	40%	21%	44%
Min	17%	79%	19%	6%	10%	88%	6%	2%	26%	35%	11%	22%
Max	35%	99%	58%	30%	24%	99%	31%	11%	75%	56%	36%	80%
AR (documented)	26%	91%	34%	5%	58%	87%	10%	6%	43%	45%	17%	63%

235

236 From the PIRA model, it can be calculated how much volume flow per hour of exposure time

237 is required to not exceed a certain PIRA. The results are shown in Figure 5. It can be seen that

238 for a PIRA of 10% a volume flow of clean air of 750 m³/h and hour of exposure has to be

239 supplied to the room (see Table 3), whereas for two hours 1500 m³/h will be necessary for the

240 same PIRA.

241 As a regression of the calculated results presented in Figure 5 equation (19) was derived.

242 Using equation (19) the required volume flow per hour of exposure time can be calculated.

243 This information refers to the steady state if the product of ACH and t is higher than 5.0, see

244 Figure 1. If the product is smaller, correspondingly lower volume flows lead to the respective

245 PIRA.
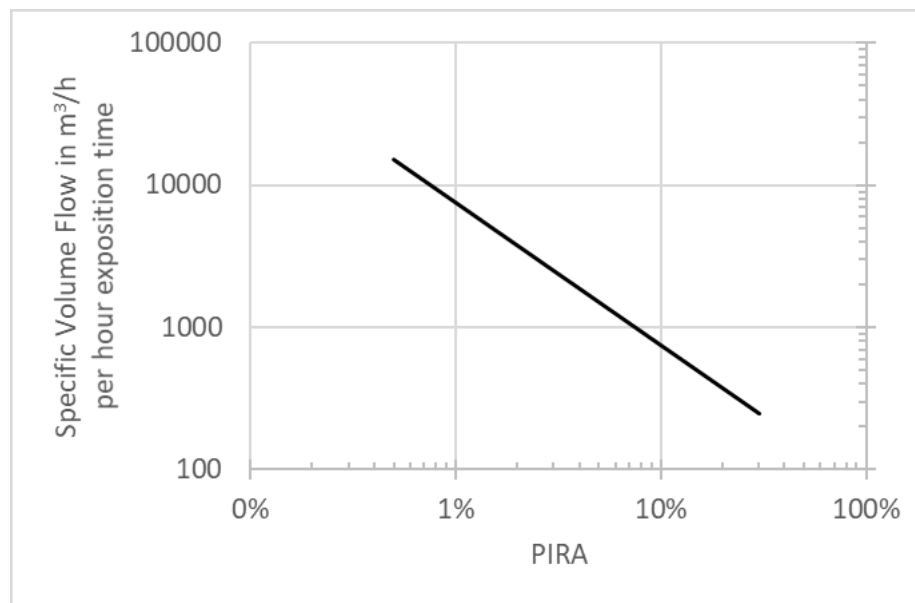
$$Q_{sp} = 75 \cdot \frac{1}{PIRA} \qquad (19)$$

Figure 5: Required specific volume flow per hour exposure time with regard to meeting a specific PIRA

Table 3 lists practical examples of the required volume flows depending on the exposure time and PIRA.

Table 3: Required volume flow at a certain exposure time for a defined PIRA

			PIRA		
			1%	5%	10%
exposure time in h		1	7500 m³/h	1500 m³/h	750 m³/h
		2	15000 m³/h	3000 m³/h	1500 m³/h
		3	22500 m³/h	4500 m³/h	2250 m³/h

Another type of evaluation shows the possible number of infected persons in relation to the person-related volume flow and the number of persons in a room (see Figure 6), if several exposed persons are in a room and each person would have 6 m³ of room volume available. If more volume flow is available to each person, the result changes marginally and tends towards a lower PIRA. For an exposure time of two hours a volume flow of 20 m³/(h·Per)

258   resulted in five probably infected persons in a room with 20, 40 or 100 persons, but of course

259   only one probably infected person in a room with two persons. For a volume flow of

260   60 m³/(h·Per) the number decreases to two probably infected persons in a room with 20, 40 or

261   100 persons, but of course stayed at one probably person for just two persons in a room.
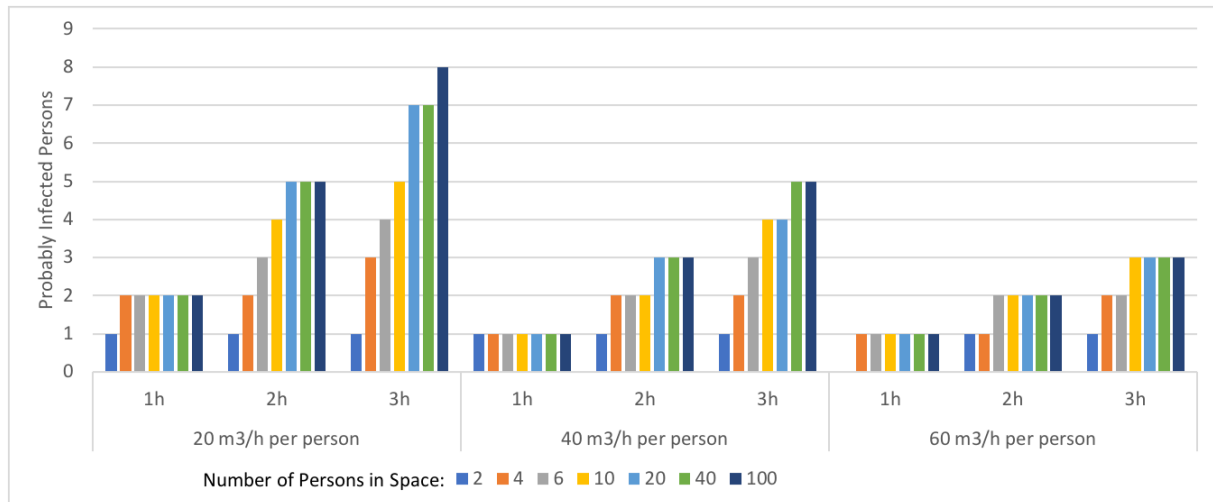

263   *Figure 6: Number of persons probably infected according to a specific volume flow*

264

Discussion

266   For the first time with a q based on R_0 the PIRA was calculated for different known SARS-

267   CoV-2 outbreaks. In addition, the necessary air volume flows to reduce the risk of infection

268   were calculated.

269   In Table 4 the q-values are compared according to the stationary equation (3) and the PIRA

270   model under the boundary conditions of Table 1. Large differences between the same

271   activities were observed in the calculation of steady-state.

272   First of all, in comparison, with fixed q according to equation (9) very good agreement can be

273   achieved with the documented AR in the retrospectively considered cases A, B, C, H, I, J, K.

274

275 *Table 4: comparison steady state and unsteady calculated quanta*

	q in 1/h											
	A	B	C	D	E	F	G	H	I	J	K	L
q steady state	255	344	275	965	67	449	808	2545	223	144	411	330
q unsteady	232	4213	139	139	139	4213	116	116	139	139	139	139

276

277 In outbreak D, the documentation does not clearly show how large the actual AR was for the

278 area under consideration. Due to the fact, that only the person who showed symptoms was

279 isolated, it is possible that in the meantime, additional persons, who were already infected by

280 the index case may have infected others (e.g. presymptomatically) leading to the high AR.

281 In outbreak E, there is only little documentation of the infection process, and further contact

282 between some of the persons has occurred in a restaurant afterwards. Furthermore, it has not

283 been determined whether the infection can be attributed to only one person. The high AR after

284 a short time of exposure allows the conclusion that either two index persons were present or

285 that the exposure time was prolonged by the meeting in a restaurant.

286 In outbreak F, the group was not together for the entire time and some of the subjects

287 continued rehearsing in another room. For this reason, the exposure time for the whole group

288 was lower and therefore this may account for the lower AR than calculated by PIRA is given.

289 In outbreak L an air exchange rate of 21 1/h was assumed. A relatively small change in the

290 assumed volume flow has a significant influence on the result of PIRA (where the total

291 exposure time was used). Furthermore, it cannot be excluded that droplet transmission may

292 also have happened.

293 Secondly, many assumptions were made, therefore it is not clear if the formula is already

294 optimal, perhaps further optimization during the course of the pandemic is possible if further

295 knowledge is available.

296   Third, the calculation model does not consider the sedimentation behavior of particles. It is

297   known that at higher air velocities and especially at high turbulence the sedimentation

298   behavior increases. In typical indoor air flows this decrease is about 10 % per hour. Compared

299   to the uncertainty of the overall emission rate, this effect is not significant.

300   Fourth, the calculation model assumes a homogeneous distribution of the particles in the room

301   air. Practically however the ventilation effectiveness is locally very different. The differences

302   can be slightly greater than 100%.

303   Finally, it must be noted that the aerosol concentration is significantly higher in the near field

304   of the emitting person and the results of PIRA are not valid within the generally accepted

305   1.5 m distance rules.

306

Conclusion

308   It was shown in this investigation that it was possible to calculate the risk of an infection via

309   aerosols for situations where the long-distance transmission is more important. By using the

310   model presented here, a good agreement to previous infection outbreaks in different settings

311   and different attack rates was achieved. Previous retrospectively determined quanta emission

312   rates usually assumed a stationary state. However, if the concentration process is important

313   for the total amount of inhaled virus-laden aerosols (usually at ACH x t < 5), then a stationary

314   observation leads to an incorrect boundary condition. The time-dependent viability of the

315   virus also plays a significant role. Here, the influence of the viability is higher at low air

316   change rates compared with high ones, because the virus stays in the room air for a longer

317   time period and the proportion of inactivated pathogens increase. However, the effect of time-

318   dependent viability is not that important that a low air change rate has an overall positive

319   effect.

320   To reduce the risk of infection via aerosols the necessary volume flow of virus-free air

321   depending on the exposure time can be seen in Figure 5. This figure may be helpful to

322   implement measures, like increasing the virus-free air supply rate. Furthermore, the number of

323   exposed persons has to be kept in mind. An infection risk of 60% may result in one infected

324   person in a two-person office, but in 60 infected persons in a room with 100 persons.

325   Predicting the infection risk via aerosols and knowing the important parameters can help in the

326   selection of appropriate preventive actions.

327

328   **Declarations**

329   The authors received no specific funding for this work.

330   The authors declare no competing interests.

331   The authors declare that they followed the appropriate research guidelines.

Literature

[1] Y. Li, H. Qian, J. Hang, X. Chen, L. Hong, P. Liang, J. Li, S. Xiao, J. Wie, L. Liu und M. Kang, „Evidence for probable aerosol transmission of SARS-CoV-2 in a poorly ventilated restaurant,“ *Preprint medXRiv,* 2020.

[2] G. Correia, L. Rodrigues, M. Gameiro da Silva und T. Gonçalves, „Airborne route and bad use of ventilation systems as non-neglible factors in SARS-CoV-2 transmission,“ *Medical Hypotheses,* Bd. 141, 2020.

[3] L. Ferretti, C. Wymant, M. Kendall, L. Zhao, A. Nurtay, L. Abeler-Dörner, M. Parker, D. Bonsall und C. Fraser, „Quantifying SARS-CoV-2 transmission suggests epidemic control with digital contact tracing,“ *Science,* Bd. eabb6936, p. 368, 2020.

[4] L. Morawska und J. Cao, „Airborne transmission of SARS-CoV-2: The world should face the reality,“ *Environment International,* Bd. 139, 2020.

[5] E. Riley, G. Murphy und R. Riley, „Airborne Spread of Measles in a Suburban Elementary School,“ *American Journal of Epidemiology,* Bd. 107, Nr. 5, pp. 421-432, 1978.

[6] W. Wells, Airborne contagion and air hygiene: an ecological study of droplet infections, 1955.

[7] C. Noakes und A. Sleigh, „Applying the Wells-Riley equation to the risk of airborne infection in hospital environments: The importance of stochastic and proximity effects,“ in *Indoor Air*, Copenhagen, Denmark, 2008.

[8] L. Gammaitoni und M. Nucci, „Using a Mathematical Model to Evaluate the Efficacy of TB Control Measures,“ *Emerging Infectious Diseases,* Bd. 3, Nr. 3, pp. 335-342, 1997.

[9] H. Dai und B. Zhao, „Association of the infection probability of COVID-19 with ventilation rates in confined spaces,“ *Building Simulations,* 2020.

[10] y. Liu, G. AA., A. Wilder-Smith und J. Rocklöv, „The reproductive number of COVID-19 is hisher compared to SARS coronavirus,“ *Journal of Travel Medicine,* pp. 1-4, 2020.

[11] Y. Alimohamadi, M. Taghdir und M. Sepandi, „The Estimate of the Basic Reproduction Number of Novel Coronavirus disease (COVID-19): A Systematic Review and Meta-Analysis,“ *Journal of Preventive Medicine and Public Health,* Bd. March, 2020.

[12] Y.-F. Lin, Q. Duan, Y. Zhou, T. Yuan, P. Li, T. Fitzpatrick, F. Leiwen, A. Feng, G. Luo, Y. Zhan, B. Liang, S. Fan, Y. Lu, B. Wang, Z. Wang, H. Zhao, Y. Gao, M. Li, D. Chen, X. Chen, Y. Ao, L. Li, W. D. X. Cai, Y. Shu und H. Zhou, „Spread and Impact of COVID-19 in China: A Systematic Review and Synthesis of Predictions From Transmission-Dynamic Models,“ *frontiers in Medicine,* 2020.

[13] S. Miller, W. Nazaroff, J. Jimenez, A. Boerstra, G. Buonanno, S. Dancer, J. Kurnitski, L. Marr, L. Morawska und C. Noakes, „Transmission of SARS-CoV-2 by inhalation of respiratory aerosol in the Skagit Valley Chorale superspreading event,“ *Preprint medXRiv,* 2020.

[14] D. Mürbe, M. Kriegel, J. Lange, H. Rotheudt und M. Fleischer, „Aerosol emission is inscreased in professional singing,“ *Preprint,* 2020.

[15] A. Hartmann, J. Lange, H. Rotheudt und M. Kriegel, „Emission rate and particle size of bioaerosols during breathing, speaking and coughing,“ *Preprint,* 2020.

[16] N. van Doremalen, T. Bushmaker, D. Morris, M. Holbrook, A. Gamble, B. Williamson, A. Tamin, J. T. N. Harcourt, S. Gerber, J. Lloyd-Smith, E. de Wit und V. Munster, „Aerosol and Surface Stability of SARS-CoV-2 as Compared with SARS-CoV-1,“ *New England Journal of Medicine,* Bde. %1 von %2April, 16, p. 382, 2020.

[17] J. Gupta, C.-H. Lin und Q. Chen, „Characterizing exhaled airflow from breathing and talking,“ *Indoor Air,* Bd. 20, pp. 31-39, 2010.

[18] A. Córdova und I. Latasa, „Respiratory flows as a method for safely preventing the coronvirus transmission (COVID-19),“ *Apunts Sports Medicine,* Bd. 55, pp. 81-85, 2020.

[19] J. Jiang, R. Hanna, M. Willey und A. Rieves, „The measurement of airflow using Singing helmet that allows free movement of the jaw,“ *Journal of Voice,* Bd. 30, Nr. 6, pp. 641-648, 2016.

[20] R. Dumond, S. Gastinger, H. Rahman, A. Le Faucheur, P. Quinton, H. Kang und J. Prioux, „Estimation of respiratory colume from thoracoabdominal breathing distances: comparison of two models of machine learning,“ *European Journal of Applied Physiology,* Bd. 117, pp. 1533-1555, 2017.

[21] B. Binazzi, B. Lanini, R. Bianchi, I. Romagnoli, M. Nerini, F. Gigliotti, R. M.-E. J. Duranti und G. Scano, „Breathing Pattern and kinematics in normal subjects during speech, singing and loud whispering,“ *Acta Physiologica,* Bd. 186, pp. 233-246, 2006.

[22] Spektrum Akademischer Verlag, Heidelberg, „Lexikon der Biologie,“ spektrum.de, 1999. [Online]. Available: https://www.spektrum.de/lexika/showpopup.php?lexikon_id=9&art_id=5744&nummer=1988. [Zugriff am 05 Oktober 2020].

[23] B. Stephens, „HVAC Filtration and the Wells-Riley approach to assessing risks of infectious airborne diseases,“ 2013.

[24] S.-C. Chen, C.-M. Liao, S.-S. Li und S.-H. You, „A Probabilistic Transmission Model to Assess Infection Risk from Mycobacterium Tuberculosis in Commercial Passenger Trains,“ *Risk Analysis,* Bd. 31, Nr. 6, pp. 930-939, 2011.

[25] G. Chowell, H. Nishiura und L. M. A. Bettencourt, „Comparative estimation of the reproduction number of pandemic influenza from daily case notification data,“ *Journal of the Royal Society Interface,* Bd. 4, pp. 155-166, 2006.

[26] B. J. Coburn und S. Blower, „Predicting the potential for within-flight transmission and global dissemination of MERS,“ *The Lancet,* Nr. 14, 2014.

[27] WHO, „WHO MERS Global Summary and Assessment of Risk,“ WHO, 2019.

[28] WHO, „Consensus document on the epidemiology of severe acute respiratory syndrome (SARS),“ WHO, 2003.

[29] G. Buonanno, L. Stabile und L. Morawska, „Estimation of airborne viral transmission: Quanta emission rate of SARS-CoV-2 for infection risk assessment,“ *Environment International,* Bd. 141, 2020.

[30] X. He, E. H. Y. Lau, P. Wu, X. Deng, J. Wang, X. Hao, Y. C. Lau, J. Y. Wong, Y. Guan, X. Tan, X. C. Y. Mo, B. Lio, W. Chen, F. Hu, Q. Zhang, M. Zhong, Y. Wu, L. Zhao, F. Zhang, C. B. J., F. Li und G. M. Leung, „Author Correction: Temporal Dynamics in viral shedding and transmissibilitiy of COVID-19,“ *Nature Medicine,* 2020.

[31] N. A. o. Sciences, The Airliner Cabin Environment and the Health of Passengers and Crew, United States of America: National Academy Press, 2002.

[32] T. Günther, M. Czech-Sioli, D. Indenbirken, A. Robitailles, P. Tenhaken, M. Exner, M. Ottinger, N. Fischer, A. Grundhoff und M. M. Brinkmann, „Investigation of a superspreading event preceding the largest meat processing plant-related SARS-Coronavirus 2 outbreak in Germany,“ *Preprint,* 2020.

[33] Y. Shen, C. Li, H. Dong, Z. Wang, L. Martinez, Z. Sun, A. Handel, Z. Chen, E. Chen, M. Ebel, F. Wang, B. Yi, H. Wang, X. Wang, A. Wang, B. Chen, Y. Qi, L. Liang, Y. Li, F. Ling, J. Chen und G. Xu, „Community Outbreak Investigation of SARS-CoV-2 Transmission Among Bus Riders in Eastern China,“ *JAMA International Medicine,* 2020.

[34] S. Park, Y.-M. Kim, S. Lee, B.-J. Na, C. Kim, J.-i. Kim, H. Kim, Y. Kim, Y. Park, I. Huh, H. Kim, H. Yoon, H. Jang, K. Kim, Y. Chang, I. Kim, H. Lee, J. Gwack, S. Kim, M. Lim, S. Kweon, Y. Choe, O. Park und E. Jeong, „Coronavirus Disease Outbreak in Call Center, South Korea," *Emerging Infectious Diseases,* Bd. 26, Nr. 8, pp. 1666-1670, 2020.

[35] C. Stein-Zamir, N. Abramson, H. Shoob, E. Libal, M. Bitan, T. Cardash, R. Cayam und I. Miskin, „A large COVID-19 outbreak in a high school 10 days after schools' reopening, Israel, May 2020," *Eurosurveillance,* 2020.

[36] J. Lu, J. Gu, K. Li, C. Xu, W. Su, Z. Lai, D. Zhou, C. Yu, B. Xu und Z. Yang, „COVID-19 Outbreak Associated with Air Conditioning in Restaurant, Guangzhou, China," *Emerging Infectious Diseases,* Bd. 26, Nr. 7, pp. 1628-1631, 2020.

[37] N. C. Khanh, P. Q. Thai, H.-L. Quach, N.-A. H. Thi, P. C. Dinh, T. N. Duong, L. T. Q. Mai, N. D. Nghia, T. T. A., L. N. Quang, T. D. Quang, T.-T. Nguyen, F. Vogt und D. D. Anh, „Transmission of Severe Acute Respiratory Syndrome Coronavirus 2 During Ling Flight," *Emerging Infectious Diseases,* Bd. 26, Nr. 11, 2020.

[38] G. Buonanno, L. Morawska und L. Stabile, „Quantitative Assessment of the Risk of Airborne Transmission of SARS-COV-2-Infection: Prospective and Retrospective Applications," *Preprint MedXRiv,* 2020.